

JYX



This is a self-archived version of an original article. This version may differ from the original in pagination and typographic details.

Author(s): ALICE Collaboration

Title: Photoproduction of $K+K^-$ Pairs in Ultraperipheral Collisions

Year: 2024

Version: Published version

Copyright: © 2024 CERN, for the ALICE Collaboration

Rights: CC BY 4.0

Rights url: <https://creativecommons.org/licenses/by/4.0/>

Please cite the original version:

ALICE Collaboration. (2024). Photoproduction of $K+K^-$ Pairs in Ultraperipheral Collisions. Physical Review Letters, 132(22), Article 222303.
<https://doi.org/10.1103/physrevlett.132.222303>

Photoproduction of K^+K^- Pairs in Ultraperipheral Collisions

S. Acharya *et al.*^{*}
(ALICE Collaboration)

 (Received 8 December 2023; revised 16 February 2024; accepted 3 May 2024; published 31 May 2024)

K^+K^- pairs may be produced in photonuclear collisions, either from the decays of photoproduced $\phi(1020)$ mesons or directly as nonresonant K^+K^- pairs. Measurements of K^+K^- photoproduction probe the couplings between the $\phi(1020)$ and charged kaons with photons and nuclear targets. The kaon-proton scattering occurs at energies far above those available elsewhere. We present the first measurement of coherent photoproduction of K^+K^- pairs on lead ions in ultraperipheral collisions using the ALICE detector, including the first investigation of direct K^+K^- production. There is significant K^+K^- production at low transverse momentum, consistent with coherent photoproduction on lead targets. In the mass range $1.1 < M_{KK} < 1.4$ GeV/ c^2 above the $\phi(1020)$ resonance, for rapidity $|y_{KK}| < 0.8$ and $p_{T,KK} < 0.1$ GeV/ c , the measured coherent photoproduction cross section is $d\sigma/dy = 3.37 \pm 0.61(\text{stat}) \pm 0.15(\text{syst})$ mb. The center-of-mass energy per nucleon of the photon-nucleus (Pb) system $W_{\gamma\text{Pb},n}$ ranges from 33 to 188 GeV, far higher than previous measurements on heavy-nucleus targets. The cross section is larger than expected for $\phi(1020)$ photoproduction alone. The mass spectrum is fit to a cocktail consisting of $\phi(1020)$ decays, direct K^+K^- photoproduction, and interference between the two. The confidence regions for the amplitude and relative phase angle for direct K^+K^- photoproduction are presented.

DOI: [10.1103/PhysRevLett.132.222303](https://doi.org/10.1103/PhysRevLett.132.222303)

Introduction.—High-energy photoproduction is an important technique for studying hadronic interactions. Ultraperipheral collisions (UPCs) of relativistic ions are a tool for studying photonuclear interactions at energies far higher than those available elsewhere [1–4]. The electromagnetic field of one nucleus forms an intense virtual-photon beam that can interact with nuclei from the opposing beam. UPC interactions occur when the impact parameter (b) between the two nuclei is large enough—e.g., b is greater than the sum of the nuclear radii—so that no obscuring hadron-hadron interactions occur.

A photon can fluctuate into a quark-antiquark pair (dipole) that scatters elastically from a target nucleus, emerging as a real vector meson [5]. The elastic scattering is mediated by the Pomeron, which is a colorless object and to lowest order, composed of two gluons. The exchange involves the quantum numbers of the vacuum, so following the vector meson dominance model, the outgoing meson has the same quantum numbers $J^{PC} = 1^{--}$ as the incident photon [6]. Alternatively, the photon can fluctuate directly into a virtual meson pair, like $\pi^+\pi^-$ or K^+K^- . One of the mesons can then scatter elastically from the target, making

the pair real. For midrapidity kaons in ALICE, the kaon-proton center-of-mass energy is 50 GeV, far higher than can be studied elsewhere. Exclusive K^+K^- production can also occur via two-photon [7] or in double-Pomeron interactions [8], but this is the first observation in the photon-Pomeron channel.

Since the channels are indistinguishable, meson pairs from the decay of vector mesons [$\rho^0 \rightarrow \pi^+\pi^-$ or $\phi(1020) \rightarrow K^+K^-$] can interfere with the directly produced pairs. The production amplitude has two terms: The resonance is described using a Breit-Wigner distribution expressed in the Jackson form, with amplitude A_ϕ , and there is, in addition, a continuum component with amplitude B_{KK} [9–11], giving

$$\frac{d\sigma}{dM_{KK}} = \left| A_\phi \frac{\sqrt{M_{KK}M_\phi\Gamma_\phi}}{M_{KK}^2 - M_\phi^2 + iM_\phi\Gamma_\phi} + B_{KK} \right|^2, \quad (1)$$

where $M_\phi = 1019.416 \pm 0.016$ MeV/ c^2 [12] and Γ_ϕ are the $\phi(1020)$ mass and mass-dependent width, respectively, with

$$\Gamma_\phi = \Gamma_0 \frac{M_\phi}{M_{KK}} \left(\frac{M_{KK}^2 - 4M_K^2}{M_\phi^2 - 4M_K^2} \right)^{3/2}. \quad (2)$$

Here, $\Gamma_0 = 4.249 \pm 0.013$ MeV/ c^2 is the native $\phi(1020)$ width, and $M_K = 493.677 \pm 0.016$ MeV/ c^2 is the kaon mass [12]. Both A_ϕ and B_{KK} are complex, but only their

^{*}Full author list given at the end of the Letter.

Published by the American Physical Society under the terms of the [Creative Commons Attribution 4.0 International license](https://creativecommons.org/licenses/by/4.0/). Further distribution of this work must maintain attribution to the author(s) and the published article's title, journal citation, and DOI. Open access publication funded by CERN.

relative phase matters. By taking A_ϕ to be real, the relative phase is encoded in B_{KK} . Far above the $\phi(1020)$ resonance (many Γ_0), the mass-dependent width rises, and the cross section declines smoothly. One difference between the K^+K^- and $\pi^+\pi^-$ systems is that the branching ratio $\phi(1020) \rightarrow K^+K^-$ is only 49.1% [12], while the ρ^0 almost always decays to $\pi^+\pi^-$. This branching ratio is included in A_ϕ . Ryskin and Shabelski considered the direct dikaon contribution to the total dikaon cross section and concluded that it should be small and with a relative phase angle near zero [13]. A later calculation predicted that the dikaon system should behave similarly to the dipions, with a small correction to the width to account for three-body $\phi(1020)$ decays [11].

The transverse momentum p_T of the meson depends on the production mechanism, so it is important in selecting coherent photoproduction events, where a dipole or virtual meson pair scatters from the target nucleus. The meson p_T is the vector sum of the photon p_T and the Pomeron p_T , which usually dominates [14]. For coherent production, its scale is controlled by the form factor of the target nucleus. Destructive interference between the amplitudes for production on the two nuclei can reduce the cross section at low p_T , especially near midrapidity [14,15]. In incoherent production, when a dipole or virtual meson pair scatters from a single nucleon, the typical p_T is larger, around a few hundred MeV/ c . Although Pomeron-Pomeron interactions can also produce exclusive K^+K^- pairs [8], because of the short range of the strong force, these reactions cannot be coherent over the entire nuclei and, so, will not produce a peak at low p_T and do not contribute to the current coherent measurement.

Previously, $\phi(1020)$ photoproduction has been studied at fixed-target experiments [6,16] and the HERA ep collider [17–19]. However, the direct K^+K^- contribution has not yet been observed. The H1 Collaboration searched for skewing in the ϕ Breit-Wigner peak due to direct K^+K^- production (in electroproduction) but found no evidence for it [19]. In contrast, the $\rho^0 +$ direct $\pi^+\pi^-$ state has been studied in both UPCs [20–25] and, at lower energy, at fixed-target experiments [6]. The $\pi^+\pi^-$ mass spectra are well fit by the sum of amplitudes for ρ^0 and direct $\pi^+\pi^-$, with a high-statistics fit exhibiting additional interference from $\omega \rightarrow \pi^+\pi^-$ [22,26]. Higher-mass $\pi^+\pi^-$ states have also been seen [23,27,28].

This Letter reports on exclusive photoproduction of the K^+K^- final state, from the decay of the $\phi(1020)$ and direct production. The data cover the mass region $1.1 < M_{KK} < 1.4$ GeV/ c^2 . This is significantly above the $\phi(1020)$ peak, with the lower mass limit at about $M_\phi + 18\Gamma_0$.

The cross sections are measured at the center-of-mass energy per nucleon of the photon-nucleus (Pb) system $W_{\gamma Pb,n}$, where $W_{\gamma Pb,n}$ varies from 33 to 188 GeV, depending on M_{KK} and rapidity. This range of energies is more than an order of magnitude higher than previous studies using heavy-nucleus targets [6,16].

Detector and data.—The results presented in this Letter are based on the data collected in 2015 by the ALICE experiment [29,30], with Pb-Pb collisions at a center-of-mass energy per nucleon pair $\sqrt{s_{NN}} = 5.02$ TeV. A dedicated trigger was used to select candidate UPC events [23], rejecting any activity within the time windows for nominal beam-beam interactions, using the scintillator detectors V0 [31] and AD [32,33] located at large positive and negative pseudorapidity. In addition, the trigger required that the silicon pixel detector (SPD), the two innermost layers of the inner tracking system (ITS) [34], measured at least two short track segments with a large opening angle in azimuth.

The time projection chamber (TPC) covering the pseudorapidity acceptance of $|\eta| < 0.9$ was used for charged particle tracking and vertexing together with the ITS as well as for particle identification based on the specific ionization energy loss, dE/dx [35].

Analysis procedure.—The analysis selected events with exactly two good tracks. The tracks were required to have at least 50 hits (clusters) in the TPC, at least one hit in each of the two layers of the SPD, and to have the distance-of-closest approach to the event vertex of less than $0.0182 + 0.035/p_T^{1.01}$ cm in the transverse plane and less than 2 cm along the beam direction. The two selected tracks having opposite charge are reconstructed as K^+K^- pair candidates under the kaon mass hypothesis. As there are no same-charge pairs passing the particle identification criteria, the contribution of uncorrelated background could be ignored in this analysis.

Kaons are identified based on the dE/dx measurement in the TPC. The selection criteria are applied to the variable n_{σ_i} , the deviation of the measured signal from the expected signal in units of the dE/dx measurement uncertainty for each particle hypothesis i . Since the ratio of signal K^+K^- pairs to background $\pi^+\pi^-$ pairs is less than 0.1%, stringent particle identification criteria are introduced. First, the tracks in each pair are required to satisfy $|n_{\sigma_K}| < 3$. In addition, the tracks which are compatible within $2n_{\sigma_{\pi,\mu,e}}$ are excluded to reject $\pi^+\pi^-$ pairs as well as dilepton pairs from the $\gamma\gamma \rightarrow l^+l^-$ process.

The contamination of the K^+K^- pair candidates by the misidentified particles is estimated from the two-dimensional n_{σ_K} distribution of the two tracks in each pair. While the signal K^+K^- pairs have a two-dimensional Gaussian-like distribution centered at (0,0), background pairs are clustered at nonzero values. For $1.1 < M_{KK} < 1.4$ GeV/ c^2 , the contamination is negligible as the signal and background distributions are well separated from each other. At higher masses, the expected difference in dE/dx between kaons and lighter particles decreases, so they become indistinguishable in some n_{σ_K} regions. Therefore, the invariant mass range above 1.4 GeV/ c^2 is not used in the analysis. For pairs with $M_{KK} < 1.1$ GeV/ c^2 , the kaons lose energy rapidly and do not reach the sensitive region of the ALICE detector.

Measurement of the cross section.—The invariant mass differential cross section of exclusive K^+K^- photoproduction is obtained by correcting the number of K^+K^- candidates (N_{KK}) found in the rapidity interval of $|y_{KK}| < 0.8$ and in the p_T interval of $p_{T,KK} < 0.1$ GeV/ c by acceptance and efficiency ($\mathcal{A} \times \varepsilon$):

$$\frac{d^2\sigma}{dM_{KK}dy_{KK}} = \frac{N_{KK} \times f_{\text{pileup}}}{(\mathcal{A} \times \varepsilon) \times \mathcal{L} \times \Delta M_{KK} \times \Delta y_{KK}}. \quad (3)$$

The $\mathcal{A} \times \varepsilon$ is computed using a dedicated Monte Carlo simulation with STARlight [36] for the K^+K^- pairs from direct production and $\phi(1020)$ decays.

The generated K^+K^- pairs are transported through the detector setup using a GEANT3 model [37] to simulate a realistic detector response. The corresponding integrated luminosity (\mathcal{L}) for the data sample is $0.406 \mu\text{b}^{-1}$ with a relative systematic uncertainty of 2.6% [38]. Some events are lost due to pileup, when another interaction creates a signal in one of the veto detectors. The pileup events mainly come from two-photon production of e^+e^- pairs, and their effect is taken into account with an additional correction factor, $f_{\text{pileup}} = 11.1 \pm 3.8\%$ [23]. Similarly, the p_T^2 -differential cross section of exclusive K^+K^- photoproduction in $1.1 < M_{KK} < 1.4$ GeV/ c^2 is measured:

$$\frac{d^2\sigma}{dp_{T,KK}^2 dy_{KK}} = \frac{N_{KK} \times f_{\text{pileup}}}{(\mathcal{A} \times \varepsilon) \times \mathcal{L} \times \Delta p_{T,KK}^2 \times \Delta y_{KK}}. \quad (4)$$

Systematic uncertainties.—The systematic uncertainties of the measured cross section are estimated for the track selection criteria (1.5%) and the track matching between ITS and TPC (4%) as well as for the acceptance and efficiency (1%), without dependence on $p_{T,KK}$, y_{KK} , and M_{KK} [23]. Uncertainties of 1% and 3.8% are included for the trigger efficiency and for the pileup correction, respectively [23]. The uncertainty of the luminosity (2.6%) results from the uncertainty of the reference luminosity in the cross section of 2.5% [38] and an additional 0.4% uncertainty on the live time of readout detectors used for the trigger.

The systematic uncertainty of the kaon identification is estimated as a function of $p_{T,KK}$ and M_{KK} to account for the track momentum dependence in the kaon identification performance. The expected signal of TPC dE/dx for each particle hypothesis is varied in the MC simulations by the maximum difference of the signal in data and MC simulations. Then, n_{σ_i} and the corresponding kaon identification efficiency are recalculated. The resulting uncertainty is negligible for $1.1 < M_{KK} < 1.2$ GeV/ c^2 and amounts to 3.9% and 6.5% for $1.2 < M_{KK} < 1.3$ GeV/ c^2 and $1.3 < M_{KK} < 1.4$ GeV/ c^2 , respectively. The systematic uncertainty increases slowly as a function of $p_{T,KK}$ from 3.4% for $p_{T,KK} < 0.025$ GeV/ c to 4.9% for $0.1 < p_{T,KK} < 0.2$ GeV/ c . Over most of the kinematic range, this is the largest single systematic uncertainty.

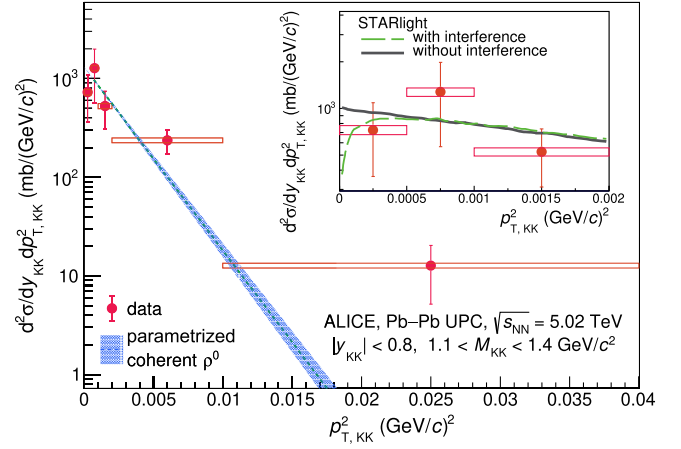


FIG. 1. Differential cross section as a function of $p_{T,KK}^2$ for exclusive K^+K^- photoproduction in Pb-Pb UPCs at $\sqrt{s_{\text{NN}}} = 5.02$ TeV and $|y_{KK}| < 0.8$. The vertical lines and boxes across the data points represent statistical and systematic uncertainties, respectively. The dashed blue line and band are the result of a fit to an exponential with the fixed slope parameter $b = 428 \pm 6(\text{stat}) \pm 15(\text{syst})$ (GeV/ c) $^{-2}$, from a previous result on ρ^0 production [39] (see the text for details). The inset shows two curves from STARlight with and without interference between the two photon directions [14,36].

Results.—Figure 1 shows the p_T^2 spectrum of the selected K^+K^- events. Most of the cross section is concentrated below $p_{T,KK}^2 < 0.01$ (GeV/ c) 2 , consistent with coherent photoproduction. Some events are seen at higher values of $p_{T,KK}^2$; these may be from incoherent production. The coherent data are well described with an exponential shape $d^2\sigma/dydp_T^2 = a \exp(-bp_T^2)$, where the slope parameter b is fixed to that measured for coherent ρ^0 photoproduction on lead, $b = 428 \pm 6(\text{stat}) \pm 15(\text{syst})$ (GeV/ c) $^{-2}$ [39]. The figure inset shows an expanded view of the low p_T^2 region and compares the data with two STARlight calculations, with and without an interference between photon emission from the two nuclei [14,36], which exhibit different trends only at very low p_T . The curve with interference is a slightly better match to the data.

The invariant mass-dependent cross section for coherent K^+K^- photoproduction is shown in Fig. 2. The data with $p_{T,KK}^2 > 0.01$ (GeV/ c) 2 are mostly from incoherent photoproduction and so are not included in the cross sections. The integrated cross section $d\sigma/dy_{KK} = 3.37 \pm 0.61(\text{stat}) \pm 0.15(\text{syst})$ mb is measured in the mass range $1.1 < M_{KK} < 1.4$ GeV/ c^2 for rapidity $|y_{KK}| < 0.8$ and $p_{T,KK}^2 < 0.01$ (GeV/ c) 2 . K^+K^- pairs could be produced by other reactions, such as $\gamma\gamma \rightarrow f_2(1270) \rightarrow K^+K^-$, but calculations indicate that the expected cross section for this process [40] estimated using STARlight [41] is a negligible fraction of the K^+K^- photoproduction cross section as illustrated in Fig. 2.

The measured cross section is fitted to a combination of $\phi(1020) \rightarrow K^+K^-$ and direct K^+K^- production according

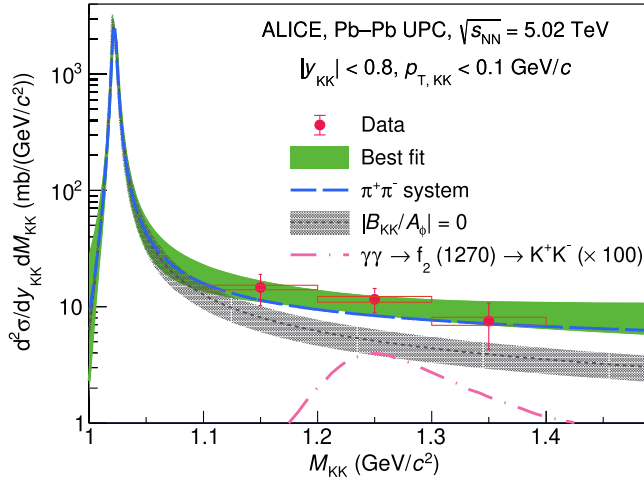


FIG. 2. Differential cross section of coherent K^+K^- photoproduction as a function M_{KK} in Pb-Pb UPCs at $\sqrt{s_{NN}} = 5.02$ TeV in $|y_{KK}| < 0.8$. The vertical lines and boxes along the data points represent statistical and systematic uncertainties, respectively. The green solid line presents the best-fit result of $|B_{KK}/A_\phi| = 0.28$ $(\text{GeV}/c^2)^{-1/2}$ and $\varphi = 0.06$ rad together with the 1σ bounds of the fit in a green band. The blue dashed curve shows the best fit with $|B_{\pi\pi}/A_\rho| = 0.54$ $(\text{GeV}/c^2)^{-1/2}$ [23] and $\varphi = 1.46$ rad (the best-fit values for ρ plus direct $\pi^+\pi^-$) [22]. The black dotted line represents the curves under the hypothesis of $|B_{KK}/A_\phi| = 0$, showing only the $\phi(1020) \rightarrow K^+K^-$ contribution. The gray band indicates the impact of the systematic uncertainty from the $\phi(1020)$ meson cross section, showing a 25% variation.

to Eq. (1). The amplitude of $\phi(1020) \rightarrow K^+K^-$ (A_ϕ) was calculated from previous photoproduction measurements on protons [16,17,42] and a Glauber calculation [41], with a branching ratio of $\phi(1020) \rightarrow K^+K^-$ ($49.2 \pm 0.5\%$) [12]. The reference $\phi(1020)$ cross sections did not include a direct K^+K^- contribution. This could have had a small effect on the measured A_ϕ .

A 25% uncertainty in A_ϕ is estimated to account for the uncertainty in the previous measurements [16,17] and the uncertainty in the Glauber approach [43]. STARlight predictions for ρ^0 production under similar circumstances were 15%–20% below the data [23], while predictions for J/ψ production were about 15%–50% above the data, depending on rapidity [44]. The latter is not surprising, since STARlight does not include gluon shadowing. The $\phi(1020)$ is intermediate in mass, but closer to the ρ^0 , so a $\pm 25\%$ uncertainty in the cross section seems conservative for the $\phi(1020)$.

The black dotted line and surrounding shaded region in Fig. 2 show the ϕ -only prediction, with the 25% uncertainty. The measured cross section is about 2.1σ above the expected $\phi(1020) \rightarrow K^+K^-$ cross section in the range $1.1 < M_{KK} < 1.4$ GeV/c^2 . Also shown, with a blue dashed line, is the prediction using the values $|B_{\pi\pi}/A_\rho| = 0.54 \pm 0.01(\text{stat}) \pm 0.02(\text{syst})$ $(\text{GeV}/c^2)^{-1/2}$ [23] and relative phase angle

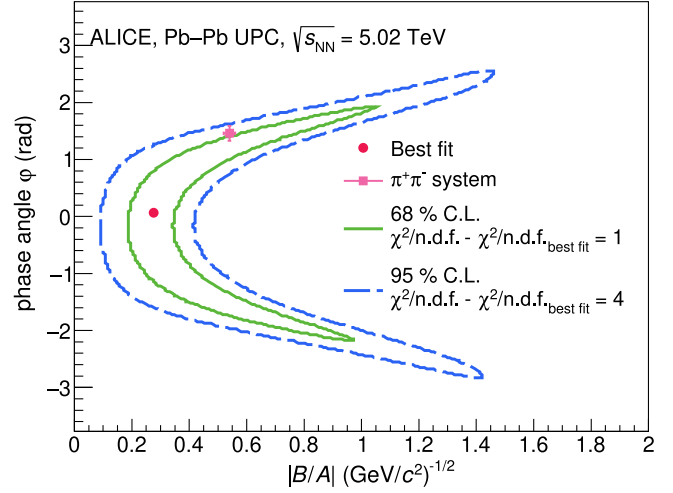


FIG. 3. Confidence regions for the relative fraction of direct K^+K^- contribution with respect to the amplitude of $\phi(1020) \rightarrow K^+K^-$ ($|B_{KK}/A_\phi|$) and the relative phase angle between $\phi(1020) \rightarrow K^+K^-$ and direct K^+K^- (φ). The best fit is shown as a red dot at $|B_{KK}/A_\phi| = 0.28$ $(\text{GeV}/c^2)^{-1/2}$ and $\varphi = 0.06$ rad found with $\chi^2/\text{n.d.f.}_{\text{best fit}} = 0.3$, while a pink square at the $|B_{\pi\pi}/A_\rho| = 0.54 \pm 0.01(\text{stat}) \pm 0.02(\text{syst})$ $(\text{GeV}/c^2)^{-1/2}$ [23] and relative phase angle $\varphi = 1.46 \pm 0.11(\text{stat}) \pm 0.07(\text{syst})$ rad [22] indicates the best-fit values for ρ plus direct $\pi^+\pi^-$. The green solid line and blue dashed line represent the boundary of 68% and 95% confidence regions, respectively.

$\varphi = 1.46 \pm 0.11(\text{stat}) \pm 0.07(\text{syst})$ rad [22] found for ρ^0 plus the direct $\pi^+\pi^-$ system. The resulting $d^2\sigma/dM_{KK}dy_{KK}$ is slightly below, but consistent with, the data points. The best fit of Eq. (1) found the relative fraction of direct K^+K^- contribution with respect to A_ϕ to be $|B_{KK}/A_\phi| = 0.28$ $(\text{GeV}/c^2)^{-1/2}$, with the relative phase angle between $\phi(1020) \rightarrow K^+K^-$ and direct K^+K^- 0.06 rad.

Figure 3 shows the confidence regions for $|B_{KK}/A_\phi|$ and φ . The horseshoe shape of the curves including the first investigation of direct K^+K^- production is because of the large correlations between the two parameters. If the interference is constructive, a small direct K^+K^- component is preferred, while a large K^+K^- component is better fit with destructive interference. The invariant mass-dependent cross section curves corresponding to the 68% confidence region are shown as a 1σ green band in Fig. 3, while the dashed blue band shows the 95% confidence level. We do not include the uncertainty on the cross section $\sigma[\gamma A \rightarrow \phi(1020)A]$ within the figure. As $\sigma[\gamma A \rightarrow \phi(1020)A]$ is reduced or increased, it moves the confidence region left or right, with relatively small changes to the shape. One standard deviation ($\pm 1\sigma$) changes in $\sigma[\gamma A \rightarrow \phi(1020)A]$ move $|B_{KK}/A_\phi|$ by about ± 0.15 $(\text{GeV}/c^2)^{-1/2}$, respectively. The best-fit point for the $\pi\pi$ system is fully compatible with the current K^+K^- measurement.

Looking ahead, during LHC run 3, ALICE will collect a far larger data sample, due to the increased luminosity [45]

and continuous-readout data acquisition system [46,47], which eliminates the need for a restrictive, prescaled trigger. Improved precision measurement of coherent K^+K^- photoproduction by the reduction of statistical uncertainty and an improved tracking will make it possible to further disentangle the resonance and nonresonance contributions with their relative phase angle.

Conclusions.—We report the first study of coherent K^+K^- photoproduction in ultraperipheral collisions at $W_{\gamma\text{pb},n}$ from 33 to 188 GeV, in the range $1.1 < M_{KK} < 1.4 \text{ GeV}/c^2$ and $|y_{KK}| < 0.8$. The $d^2\sigma/dp_{T,KK}^2 dy_{KK}$ is concentrated below $p_{T,KK}^2 < 0.01 \text{ (GeV}/c)^2$, consistent with coherent photoproduction. The measured $d^2\sigma/dM_{KK} dy_{KK}$ below $p_{T,KK}^2 < 0.01 \text{ (GeV}/c)^2$ is about 2.1σ larger than what is expected from $\phi(1020)$ production alone estimated based on HERA data with a Glauber model calculation but is consistent with a mixture of $\phi(1020)$ and direct K^+K^- production. The fitted ratio of $\phi(1020)$ production to K^+K^- production is consistent with that seen for the ρ^0 and direct $\pi^+\pi^-$.

The ALICE Collaboration thanks all its engineers and technicians for their invaluable contributions to the construction of the experiment and the CERN accelerator teams for the outstanding performance of the LHC complex. The ALICE Collaboration gratefully acknowledges the resources and support provided by all Grid centers and the Worldwide LHC Computing Grid (WLCG) Collaboration. The ALICE Collaboration acknowledges the following funding agencies for their support in building and running the ALICE detector: A. I. Alikhanyan National Science Laboratory (Yerevan Physics Institute) Foundation (ANSL), State Committee of Science and World Federation of Scientists (WFS), Armenia; Austrian Academy of Sciences, Austrian Science Fund (FWF) [grant DOI: 10.55776/M2467-N36], and Nationalstiftung für Forschung, Technologie und Entwicklung, Austria; Ministry of Communications and High Technologies, National Nuclear Research Center, Azerbaijan; Conselho Nacional de Desenvolvimento Científico e Tecnológico (CNPq), Financiadora de Estudos e Projetos (Finep), Fundação de Amparo à Pesquisa do Estado de São Paulo (FAPESP), and Universidade Federal do Rio Grande do Sul (UFRGS), Brazil; Bulgarian Ministry of Education and Science, within the National Roadmap for Research Infrastructures 2020–2027 (object CERN), Bulgaria; Ministry of Education of China (MOEC), Ministry of Science and Technology of China (MSTC), and National Natural Science Foundation of China (NSFC), China; Ministry of Science and Education and Croatian Science Foundation, Croatia; Centro de Aplicaciones Tecnológicas y Desarrollo Nuclear (CEADEN), Cubaenergía, Cuba; Ministry of Education, Youth and Sports of the Czech Republic, Czech Republic; The Danish Council for Independent Research | Natural

Sciences, the VILLUM FONDEN, and Danish National Research Foundation (DNRF), Denmark; Helsinki Institute of Physics (HIP), Finland; Commissariat à l’Energie Atomique (CEA) and Institut National de Physique Nucléaire et de Physique des Particules (IN2P3) and Centre National de la Recherche Scientifique (CNRS), France; Bundesministerium für Bildung und Forschung (BMBF) and GSI Helmholtzzentrum für Schwerionenforschung GmbH, Germany; General Secretariat for Research and Technology, Ministry of Education, Research and Religions, Greece; National Research, Development and Innovation Office, Hungary; Department of Atomic Energy Government of India (DAE), Department of Science and Technology, Government of India (DST), University Grants Commission, Government of India (UGC), and Council of Scientific and Industrial Research (CSIR), India; National Research and Innovation Agency—BRIN, Indonesia; Istituto Nazionale di Fisica Nucleare (INFN), Italy; Japanese Ministry of Education, Culture, Sports, Science and Technology (MEXT) and Japan Society for the Promotion of Science (JSPS) KAKENHI, Japan; Consejo Nacional de Ciencia (CONACYT) y Tecnología, through Fondo de Cooperación Internacional en Ciencia y Tecnología (FONCICYT) and Dirección General de Asuntos del Personal Académico (DGAPA), Mexico; Nederlandse Organisatie voor Wetenschappelijk Onderzoek (NWO), Netherlands; The Research Council of Norway, Norway; Commission on Science and Technology for Sustainable Development in the South (COMSATS), Pakistan; Pontificia Universidad Católica del Perú, Peru; Ministry of Education and Science, National Science Centre, and WUT ID-UB, Poland; Korea Institute of Science and Technology Information and National Research Foundation of Korea (NRF), Republic of Korea; Ministry of Education and Scientific Research, Institute of Atomic Physics, Ministry of Research and Innovation, and Institute of Atomic Physics and Universitatea Nationala de Stiinta si Tehnologie Politehnica Bucuresti, Romania; Ministry of Education, Science, Research and Sport of the Slovak Republic, Slovakia; National Research Foundation of South Africa, South Africa; Swedish Research Council (VR) and Knut and Alice Wallenberg Foundation (KAW), Sweden; European Organization for Nuclear Research, Switzerland; Suranaree University of Technology (SUT), National Science and Technology Development Agency (NSTDA), and National Science, Research and Innovation Fund (NSRF via PMU-B B05F650021), Thailand; Turkish Energy, Nuclear and Mineral Research Agency (TENMAK), Turkey; National Academy of Sciences of Ukraine, Ukraine; Science and Technology Facilities Council (STFC), United Kingdom; National Science Foundation (NSF) and U.S. Department of Energy, Office of Nuclear Physics (DOE NP), USA. In addition,

individual groups or members have received support from: Czech Science Foundation (Grant No. 23-07499S), Czech Republic; European Research Council, Strong 2020—Horizon 2020 (Grants No. 950692 and No. 824093), European Union; ICSC—Centro Nazionale di Ricerca in High Performance Computing, Big Data and Quantum Computing, European Union—NextGenerationEU; and Academy of Finland (Center of Excellence in Quark Matter) (Grants No. 346327 and No. 346328), Finland.

-
- [1] C. A. Bertulani, S. R. Klein, and J. Nystrand, Physics of ultra-peripheral nuclear collisions, *Annu. Rev. Nucl. Part. Sci.* **55**, 271 (2005).
- [2] A. J. Baltz, The physics of ultraperipheral collisions at the LHC, *Phys. Rep.* **458**, 1 (2008).
- [3] J. G. Contreras and J. D. Tapia Takaki, Ultra-peripheral heavy-ion collisions at the LHC, *Int. J. Mod. Phys. A* **30**, 1542012 (2015).
- [4] S. Klein and P. Steinberg, Photonuclear and two-photon interactions at high-energy nuclear colliders, *Annu. Rev. Nucl. Part. Sci.* **70**, 323 (2020).
- [5] S. R. Klein and H. Mäntysaari, Imaging the nucleus with high-energy photons, *Nat. Rev. Phys.* **1**, 662 (2019).
- [6] T. H. Bauer, R. D. Spital, D. R. Yennie, and F. M. Pipkin, The hadronic properties of the photon in high-energy interactions, *Rev. Mod. Phys.* **50**, 261 (1978); **51**, 407(E) (1979).
- [7] A. Heister *et al.* (ALEPH Collaboration), Exclusive production of pion and kaon meson pairs in two photon collisions at LEP, *Phys. Lett. B* **569**, 140 (2003).
- [8] J. Adam *et al.* (STAR Collaboration), Measurement of the central exclusive production of charged particle pairs in proton-proton collisions at $\sqrt{s} = 200$ GeV with the STAR detector at RHIC, *J. High Energy Phys.* **07** (2020) 178.
- [9] P. Söding, On the apparent shift of the rho meson mass in photoproduction, *Phys. Lett.* **19**, 702 (1966).
- [10] J. D. Jackson, Remarks on the phenomenological analysis of resonances, *Nuovo Cimento* **34**, 1644 (1964).
- [11] P. Lebiedowicz, O. Nachtmann, and A. Szczurek, Towards a complete study of central exclusive production of K^+K^- pairs in proton-proton collisions within the tensor Pomeron approach, *Phys. Rev. D* **98**, 014001 (2018).
- [12] R. L. Workman *et al.* (Particle Data Group), Review of particle physics, *Prog. Theor. Exp. Phys.* **2022**, 083C01 (2022).
- [13] M. G. Ryskin and Y. M. Shabelski, Elastic ρ' and ϕ meson photoproduction and electroproduction with nonresonant background, *Phys. At. Nucl.* **62**, 980 (1999), <https://inspirehep.net/literature/452609>.
- [14] S. R. Klein and J. Nystrand, Interference in exclusive vector meson production in heavy ion collisions, *Phys. Rev. Lett.* **84**, 2330 (2000).
- [15] B. I. Abelev *et al.* (STAR Collaboration), Observation of two-source interference in the photoproduction reaction $\text{Au Au} \rightarrow \text{Au Au } \rho^0$, *Phys. Rev. Lett.* **102**, 112301 (2009).
- [16] R. M. Eglyoff *et al.*, Measurements of elastic ρ and ϕ meson photoproduction cross-sections on protons from 30 GeV to 180 GeV, *Phys. Rev. Lett.* **43**, 657 (1979).
- [17] M. Derrick *et al.* (ZEUS Collaboration), Measurement of elastic ϕ photoproduction at HERA, *Phys. Lett. B* **377**, 259 (1996).
- [18] S. Chekanov *et al.* (ZEUS Collaboration), Exclusive electroproduction of ϕ mesons at HERA, *Nucl. Phys.* **B718**, 3 (2005).
- [19] F. D. Aaron *et al.* (H1 Collaboration), Diffractive Electroproduction of ρ and ϕ mesons at HERA, *J. High Energy Phys.* **05** (2010) 032.
- [20] C. Adler *et al.* (STAR Collaboration), Coherent ρ^0 production in ultraperipheral heavy ion collisions, *Phys. Rev. Lett.* **89**, 272302 (2002).
- [21] B. I. Abelev *et al.* (STAR Collaboration), ρ^0 photoproduction in ultraperipheral relativistic heavy ion collisions at $\sqrt{s_{NN}} = 200$ GeV, *Phys. Rev. C* **77**, 034910 (2008).
- [22] L. Adamczyk *et al.* (STAR Collaboration), Coherent diffractive photoproduction of ρ^0 mesons on gold nuclei at 200 GeV/nucleon-pair at the relativistic heavy ion collider, *Phys. Rev. C* **96**, 054904 (2017).
- [23] S. Acharya *et al.* (ALICE Collaboration), Coherent photoproduction of ρ^0 vector mesons in ultra-peripheral Pb-Pb collisions at $\sqrt{s_{NN}} = 5.02$ TeV, *J. High Energy Phys.* **06** (2020) 035.
- [24] S. Acharya *et al.* (ALICE Collaboration), First measurement of coherent ρ^0 photoproduction in ultra-peripheral Xe-Xe collisions at $\sqrt{s_{NN}} = 5.44$ TeV, *Phys. Lett. B* **820**, 136481 (2021).
- [25] A. M. Sirunyan *et al.* (CMS Collaboration), Measurement of exclusive $\rho(770)^0$ photoproduction in ultraperipheral pPb collisions at $\sqrt{s_{NN}} = 5.02$ TeV, *Eur. Phys. J. C* **79**, 702 (2019).
- [26] V. Andreev *et al.* (H1 Collaboration), Measurement of exclusive $\pi^+\pi^-$ and ρ^0 meson photoproduction at HERA, *Eur. Phys. J. C* **80**, 1189 (2020).
- [27] H. Abramowicz *et al.* (ZEUS Collaboration), Exclusive electroproduction of two pions at HERA, *Eur. Phys. J. C* **72**, 1869 (2012).
- [28] S. R. Klein (STAR Collaboration), Ultra-peripheral collisions with gold ions in STAR, *Proc. Sci.*, DIS2016 (2016) 188 [arXiv:1606.02754].
- [29] K. Aamodt *et al.* (ALICE Collaboration), The ALICE experiment at the CERN LHC, *J. Instrum.* **3**, S08002 (2008).
- [30] B. B. Abelev *et al.* (ALICE Collaboration), Performance of the ALICE experiment at the CERN LHC, *Int. J. Mod. Phys. A* **29**, 1430044 (2014).
- [31] E. Abbas *et al.* (ALICE Collaboration), Performance of the ALICE VZERO system, *J. Instrum.* **8**, P10016 (2013).
- [32] K. Akiba *et al.* (LHC Forward Physics Working Group), LHC forward physics, *J. Phys. G* **43**, 110201 (2016).
- [33] M. Broz *et al.*, Performance of ALICE AD modules in the CERN PS test beam, *J. Instrum.* **16**, P01017 (2021).
- [34] K. Aamodt *et al.* (ALICE Collaboration), Alignment of the ALICE inner tracking system with cosmic-ray tracks, *J. Instrum.* **5**, P03003 (2010).

- [35] J. Alme *et al.*, The ALICE TPC, a large 3-dimensional tracking device with fast readout for ultra-high multiplicity events, *Nucl. Instrum. Methods Phys. Res., Sect. A* **622**, 316 (2010).
- [36] S. R. Klein, J. Nystrand, J. Seger, Y. Gorbunov, and J. Butterworth, STARlight: A Monte Carlo simulation program for ultra-peripheral collisions of relativistic ions, *Comput. Phys. Commun.* **212**, 258 (2017).
- [37] R. Brun, F. Bruyant, F. Carminati, S. Giani, M. Maire, A. McPherson, G. Patrick, and L. Urban, *GEANT: Detector Description and Simulation Tool; Oct 1994*, CERN Program Library (CERN, Geneva, 1993), Long Writeup W5013, <https://cds.cern.ch/record/1082634>.
- [38] S. Acharya *et al.* (ALICE Collaboration), ALICE luminosity determination for Pb-Pb collisions at $\sqrt{s_{NN}} = 5.02$ TeV, *J. Instrum.* **19**, P02039 (2024).
- [39] J. Adam *et al.* (ALICE Collaboration), Coherent ρ^0 photoproduction in ultra-peripheral Pb-Pb collisions at $\sqrt{s_{NN}} = 2.76$ TeV, *J. High Energy Phys.* **09** (2015) 095.
- [40] A. J. Baltz, Y. Gorbunov, S. R. Klein, and J. Nystrand, Two-photon interactions with nuclear breakup in relativistic heavy ion collisions, *Phys. Rev. C* **80**, 044902 (2009).
- [41] S. R. Klein and J. Nystrand, Exclusive vector meson production in relativistic heavy ion collisions, *Phys. Rev. C* **60**, 014903 (1999).
- [42] J. A. Crittenden, Exclusive production of neutral vector mesons at the electron—proton collider HERA, [arXiv:hep-ex/9704009](https://arxiv.org/abs/hep-ex/9704009).
- [43] L. Frankfurt, V. Guzey, M. Strikman, and M. Zhalov, Nuclear shadowing in photoproduction of ρ mesons in ultraperipheral nucleus collisions at RHIC and the LHC, *Phys. Lett. B* **752**, 51 (2016).
- [44] S. Acharya *et al.* (ALICE Collaboration), Coherent J/ψ and ψ' photoproduction at midrapidity in ultra-peripheral Pb-Pb collisions at $\sqrt{s_{NN}} = 5.02$ TeV, *Eur. Phys. J. C* **81**, 712 (2021).
- [45] Z. Citron *et al.*, Report from Working Group 5: Future physics opportunities for high-density QCD at the LHC with heavy-ion and proton beams, *CERN Yellow Rep. Monogr.* **7**, 1159 (2019).
- [46] P. Buncic, M. Krzewicki, and P. Vande Vyvre, Technical design report for the upgrade of the online-offline computing system, Technical Report No: CERN-LHCC-2015-006, 2015, <https://cds.cern.ch/record/2011297>.
- [47] ALICE Collaboration, Upgrade of the ALICE time projection chamber, Technical Report No. CERN-LHCC-2013-020, 2013, <https://cds.cern.ch/record/1622286>.

S. Acharya¹²⁸, D. Adamová⁸⁷, G. Aglieri Rinella³³, M. Agnello³⁰, N. Agrawal⁵², Z. Ahammed¹³⁶, S. Ahmad¹⁶, S. U. Ahn⁷², I. Ahuja³⁸, A. Akindinov¹⁴², M. Al-Turany⁹⁸, D. Aleksandrov¹⁴², B. Alessandro⁵⁷, H. M. Alfanda⁶, R. Alfaro Molina⁶⁸, B. Ali¹⁶, A. Alici²⁶, N. Alizadehvandchali¹¹⁷, A. Alkin³³, J. Alme²¹, G. Alocco⁵³, T. Alt⁶⁵, A. R. Altamura⁵¹, I. Altsybeev⁹⁶, J. R. Alvarado⁴⁵, M. N. Anaam⁶, C. Andrei⁴⁶, N. Andreou¹¹⁶, A. Andronic¹²⁷, E. Andronov¹⁴², V. Anguelov⁹⁵, F. Antinori⁵⁵, P. Antonioli⁵², N. Apadula⁷⁵, L. Apechetché¹⁰⁴, H. Appelshäuser⁶⁵, C. Arata⁷⁴, S. Arcelli²⁶, M. Aresti²³, R. Arnaldi⁵⁷, J. G. M. C. A. Arneiro¹¹¹, I. C. Arsene²⁰, M. Arslanok¹³⁹, A. Augustinus³³, R. Averbeck⁹⁸, M. D. Azmi¹⁶, H. Baba¹²⁵, A. Badalà⁵⁴, J. Bae¹⁰⁵, Y. W. Baek⁴¹, X. Bai¹²¹, R. Bailhache⁶⁵, Y. Bailung⁴⁹, R. Bala⁹², A. Balbino³⁰, A. Baldisseri¹³¹, B. Balis², D. Banerjee⁴, Z. Banoo⁹², F. Barile³², L. Barioglio⁹⁶, M. Barlou⁷⁹, B. Barman⁴², G. G. Barnaföldi⁴⁷, L. S. Barnby⁸⁶, E. Barreau¹⁰⁴, V. Barret¹²⁸, L. Barreto¹¹¹, C. Bartels¹²⁰, K. Barth³³, E. Bartsch⁶⁵, N. Bastid¹²⁸, S. Basu⁷⁶, G. Batigne¹⁰⁴, D. Battistini⁹⁶, B. Batyunya¹⁴³, D. Bauri⁴⁸, J. L. Bazo Alba¹⁰², I. G. Bearden⁸⁴, C. Beattie¹³⁹, P. Becht⁹⁸, D. Behera⁴⁹, I. Belikov¹³⁰, A. D. C. Bell Hechavarria¹²⁷, F. Bellini²⁶, R. Bellwied¹¹⁷, S. Belokurova¹⁴², L. G. E. Beltran¹¹⁰, Y. A. V. Beltran⁴⁵, G. Bencedi⁴⁷, S. Beole²⁵, Y. Berdnikov¹⁴², A. Berdnikova⁹⁵, L. Bergmann⁹⁵, M. G. Besoiu⁶⁴, L. Betev³³, P. P. Bhaduri¹³⁶, A. Bhasin⁹², M. A. Bhat⁴, B. Bhattacharjee⁴², L. Bianchi²⁵, N. Bianchi⁵⁰, J. Bielčík³⁶, J. Bielčíková⁸⁷, A. P. Bigot¹³⁰, A. Bilandzic⁹⁶, G. Biro⁴⁷, S. Biswas⁴, N. Bize¹⁰⁴, J. T. Blair¹⁰⁹, D. Blau¹⁴², M. B. Blidaru⁹⁸, N. Bluhme³⁹, C. Blume⁶⁵, G. Boca^{22,56}, F. Bock⁸⁸, T. Bodova²¹, S. Boi²³, J. Bok¹⁷, L. Boldizsár⁴⁷, M. Bombara³⁸, P. M. Bond³³, G. Bonomi^{56,135}, H. Borel¹³¹, A. Borissov¹⁴², A. G. Borquez Carcamo⁹⁵, H. Bossi¹³⁹, E. Botta²⁵, Y. E. M. Bouziani⁶⁵, L. Bratrud⁶⁵, P. Braun-Munzinger⁹⁸, M. Bregant¹¹¹, M. Broz³⁶, G. E. Bruno^{32,97}, M. D. Buckland²⁴, D. Budnikov¹⁴², H. Buesching⁶⁵, S. Bufalino³⁰, P. Buhler¹⁰³, N. Burmasov¹⁴², Z. Buthelezi^{69,124}, A. Bylinkin²¹, S. A. Bysiak¹⁰⁸, J. C. Cabanillas Noris¹¹⁰, M. Cai⁶, H. Caines¹³⁹, A. Caliva²⁹, E. Calvo Villar¹⁰², J. M. M. Camacho¹¹⁰, P. Camerini²⁴, F. D. M. Canedo¹¹¹, S. L. Cantway¹³⁹, M. Carabas¹¹⁴, A. A. Carballo³³, F. Carnesecchi³³, R. Caron¹²⁹, L. A. D. Carvalho¹¹¹, J. Castillo Castellanos¹³¹, F. Catalano^{25,33}, C. Ceballos Sanchez¹⁴³, I. Chakaberia⁷⁵, P. Chakraborty⁴⁸, S. Chandra¹³⁶, S. Chapeland³³, M. Chartier¹²⁰, S. Chattopadhyay¹³⁶, S. Chattopadhyay¹⁰⁰, T. Cheng^{6,98}

C. Cheshkov¹²⁹ B. Cheynis¹²⁹ V. Chibante Barroso³³ D. D. Chinellato¹¹² E. S. Chizzali^{96,b} J. Cho⁵⁹ S. Cho⁵⁹ P. Chochula³³ D. Choudhury⁴² P. Christakoglou⁸⁵ C. H. Christensen⁸⁴ P. Christiansen⁷⁶ T. Chujo¹²⁶ M. Ciacco³⁰ C. Cicalo⁵³ M. R. Ciupek⁹⁸ G. Clai^{52,c} F. Colamaria⁵¹ J. S. Colburn¹⁰¹ D. Colella^{32,97} M. Colocci²⁶ M. Concas³³ G. Conesa Balbastre⁷⁴ Z. Conesa del Valle¹³² G. Contin²⁴ J. G. Contreras³⁶ M. L. Coquet¹³¹ P. Cortese^{57,134} M. R. Cosentino¹¹³ F. Costa³³ S. Costanza^{22,56} C. Cot¹³² J. Crkovská⁹⁵ P. Crochet¹²⁸ R. Cruz-Torres⁷⁵ P. Cui⁶ A. Dainese⁵⁵ M. C. Danisch⁹⁵ A. Danu⁶⁴ P. Das⁸¹ P. Das⁴ S. Das⁴ A. R. Dash¹²⁷ S. Dash⁴⁸ A. De Caro²⁹ G. de Cataldo⁵¹ J. de Cuveland³⁹ A. De Falco²³ D. De Gruttola²⁹ N. De Marco⁵⁷ C. De Martin²⁴ S. De Pasquale²⁹ R. Deb¹³⁵ R. Del Grande⁹⁶ L. Dello Stritto^{29,33} W. Deng⁶ P. Dhankher¹⁹ D. Di Bari³² A. Di Mauro³³ B. Diab¹³¹ R. A. Diaz^{7,143} T. Dietel¹¹⁵ Y. Ding⁶ J. Ditzel⁶⁵ R. Divià³³ D. U. Dixit¹⁹ Ø. Djuvsland²¹ U. Dmitrieva¹⁴² A. Dobrin⁶⁴ B. Dönigus⁶⁵ J. M. Dubinski¹³⁷ A. Dubla⁹⁸ S. Dudi⁹¹ P. Dupieux¹²⁸ M. Durkac¹⁰⁷ N. Dzalaiova¹³ T. M. Eder¹²⁷ R. J. Ehlers⁷⁵ F. Eisenhut⁶⁵ R. Ejima⁹³ D. Elia⁵¹ B. Erazmus¹⁰⁴ F. Ercolessi²⁶ B. Espagnon¹³² G. Eulisse³³ D. Evans¹⁰¹ S. Evdokimov¹⁴² L. Fabbietti⁹⁶ M. Faggin²⁸ J. Faivre⁷⁴ F. Fan⁶ W. Fan⁷⁵ A. Fantoni⁵⁰ M. Fasel⁸⁸ A. Feliciello⁵⁷ G. Feofilov¹⁴² A. Fernández Téllez⁴⁵ L. Ferrandi¹¹¹ M. B. Ferrer³³ A. Ferrero¹³¹ C. Ferrero^{57,d} A. Ferretti²⁵ V. J. G. Feuillard⁹⁵ V. Filova³⁶ D. Finogeev¹⁴² F. M. Fionda⁵³ E. Flatland³³ F. Flor¹¹⁷ A. N. Flores¹⁰⁹ S. Foertsch⁶⁹ I. Fokin⁹⁵ S. Fokin¹⁴² E. Fragiaco⁵⁸ E. Frajna⁴⁷ U. Fuchs³³ N. Funicello²⁹ C. Furget⁷⁴ A. Furs¹⁴² T. Fusayasu⁹⁹ J. J. Gaardhøje⁸⁴ M. Gagliardi²⁵ A. M. Gago¹⁰² T. Gahlaut⁴⁸ C. D. Galvan¹¹⁰ D. R. Gangadharan¹¹⁷ P. Ganoti⁷⁹ C. Garabatos⁹⁸ T. García Chávez⁴⁵ E. Garcia-Solis⁹ C. Gargiulo³³ P. Gasik⁹⁸ A. Gautam¹¹⁹ M. B. Gay Ducati⁶⁷ M. Germain¹⁰⁴ A. Ghimouz¹²⁶ C. Ghosh¹³⁶ M. Giacalone⁵² G. Gioachin³⁰ P. Giubellino^{57,98} P. Giubilato²⁸ A. M. C. Glaenger¹³¹ P. Glässel⁹⁵ E. Glimos¹²³ D. J. Q. Goh⁷⁷ V. Gonzalez¹³⁸ P. Gordeev¹⁴² M. Gorgon² K. Goswami⁴⁹ S. Gotovac³⁴ V. Grabski⁶⁸ L. K. Graczykowski¹³⁷ E. Grecka⁸⁷ A. Grelli⁶⁰ C. Grigoras³³ V. Grigoriev¹⁴² S. Grigoryan^{1,143} F. Grosa³³ J. F. Grosse-Oetringhaus³³ R. Grosso⁹⁸ D. Grund³⁶ N. A. Grunwald⁹⁵ G. G. Guardiano¹¹² R. Guernane⁷⁴ M. Guilbaud¹⁰⁴ K. Gulbrandsen⁸⁴ T. Gündem⁶⁵ T. Gunji¹²⁵ W. Guo⁶ A. Gupta⁹² R. Gupta⁹² R. Gupta⁴⁹ K. Gwizdziel¹³⁷ L. Gyulai⁴⁷ C. Hadjidakis¹³² F. U. Haider⁹² S. Haidlova³⁶ M. Haldar⁴ H. Hamagaki⁷⁷ A. Hamdi⁷⁵ Y. Han¹⁴⁰ B. G. Hanley¹³⁸ R. Hannigan¹⁰⁹ J. Hansen⁷⁶ J. W. Harris¹³⁹ A. Harton⁹ M. V. Hartung⁶⁵ H. Hassan¹¹⁸ D. Hatzifotiadou⁵² P. Hauer⁴³ L. B. Havener¹³⁹ E. Hellbär⁹⁸ H. Helstrup³⁵ M. Hemmer⁶⁵ T. Herman³⁶ G. Herrera Corral⁸ F. Herrmann¹²⁷ S. Herrmann¹²⁹ K. F. Hetland³⁵ B. Heybeck⁶⁵ H. Hillemanns³³ B. Hippolyte¹³⁰ F. W. Hoffmann⁷¹ B. Hofman⁶⁰ G. H. Hong¹⁴⁰ M. Horst⁹⁶ A. Horzyk² Y. Hou⁶ P. Hristov³³ C. Hughes¹²³ P. Huhn⁶⁵ L. M. Huhta¹¹⁸ T. J. Humanic⁸⁹ A. Hutson¹¹⁷ D. Hutter³⁹ M. C. Hwang¹⁹ R. Ilkaev¹⁴² H. Ilyas¹⁴ M. Inaba¹²⁶ G. M. Innocenti³³ M. Ippolitov¹⁴² A. Isakov^{85,87} T. Isidori¹¹⁹ M. S. Islam¹⁰⁰ M. Ivanov¹³ M. Ivanov⁹⁸ V. Ivanov¹⁴² K. E. Iversen⁷⁶ M. Jablonski² B. Jacak^{19,75} N. Jacazio²⁶ P. M. Jacobs⁷⁵ S. Jadlovská¹⁰⁷ J. Jadlovsky¹⁰⁷ S. Jaelani⁸³ C. Jahnke¹¹¹ M. J. Jakubowska¹³⁷ M. A. Janik¹³⁷ T. Janson⁷¹ S. Ji¹⁷ S. Jia¹⁰ A. A. P. Jimenez⁶⁶ F. Jonas^{75,88,127} D. M. Jones¹²⁰ J. M. Jowett^{33,98} J. Jung⁶⁵ M. Jung⁶⁵ A. Junique³³ A. Jusko¹⁰¹ J. Kaewjai¹⁰⁶ P. Kalinak⁶¹ A. S. Kalteyer⁹⁸ A. Kalweit³³ A. Karasu Uysal^{73,e} D. Karatovic⁹⁰ O. Karavichev¹⁴² T. Karavicheva¹⁴² P. Karczmarczyk¹³⁷ E. Karpechev¹⁴² M. J. Karwowska^{33,137} U. Keschull⁷¹ R. Keidel¹⁴¹ D. L. D. Keijdener⁶⁰ M. Keil³³ B. Ketzer⁴³ S. S. Khade⁴⁹ A. M. Khan¹²¹ S. Khan¹⁶ A. Khanzadeev¹⁴² Y. Kharlov¹⁴² A. Khatun¹¹⁹ A. Khuntia³⁶ Z. Khuranova⁶⁵ B. Kileng³⁵ B. Kim¹⁰⁵ C. Kim¹⁷ D. J. Kim¹¹⁸ E. J. Kim⁷⁰ J. Kim¹⁴⁰ J. Kim⁵⁹ J. Kim⁷⁰ M. Kim¹⁹ S. Kim¹⁸ T. Kim¹⁴⁰ K. Kimura⁹³ S. Kirsch⁶⁵ I. Kisel³⁹ S. Kiselev¹⁴² A. Kisiel¹³⁷ J. P. Kitowski² J. L. Klay⁵ J. Klein³³ S. Klein⁷⁵ C. Klein-Bösing¹²⁷ M. Kleiner⁶⁵ T. Klemenz⁹⁶ A. Kluge³³ C. Kobdaj¹⁰⁶ T. Kollegger⁹⁸ A. Kondratyev¹⁴³ N. Kondratyeva¹⁴² J. König⁶⁵ S. A. Königstorfer⁹⁶ P. J. Konopka³³ G. Kornakov¹³⁷ M. Korwieser⁹⁶ S. D. Koryciak² A. Kotliarov⁸⁷ N. Kovacic⁹⁰ V. Kovalenko¹⁴² M. Kowalski¹⁰⁸ V. Kozuharov³⁷ I. Králik⁶¹ A. Kravčáková³⁸ L. Krcal^{33,39} M. Krivda^{61,101} F. Krizek⁸⁷ K. Krizkova Gajdosova³³ M. Kroesen⁹⁵ M. Krüger⁶⁵ D. M. Krupova³⁶ E. Kryshen¹⁴² V. Kučera⁵⁹ C. Kuhn¹³⁰ P. G. Kuijjer⁸⁵ T. Kumaoka¹²⁶ D. Kumar¹³⁶ L. Kumar⁹¹ N. Kumar⁹¹ S. Kumar³² S. Kundu³³ P. Kurashvili⁸⁰ A. Kurepin¹⁴² A. B. Kurepin¹⁴² A. Kuryakin¹⁴² S. Kushpil⁸⁷ V. Kuskov¹⁴² M. Kutyla¹³⁷ M. J. Kwon⁵⁹ Y. Kwon¹⁴⁰ S. L. La Pointe³⁹ P. La Rocca²⁷ A. Lakrathok¹⁰⁶ M. Lamanna³³ A. R. Landou⁷⁴

R. Langoy¹²² P. Larionov³³ E. Laudi³³ L. Lautner^{33,96} R. Lavicka¹⁰³ R. Lea^{56,135} H. Lee¹⁰⁵ I. Legrand⁴⁶
G. Legras¹²⁷ J. Lehrbach³⁹ T. M. Lelek² R. C. Lemmon⁸⁶ I. León Monzón¹¹⁰ M. M. Lesch⁹⁶ E. D. Lesser¹⁹
P. Lévai⁴⁷ X. Li¹⁰ B. E. Liang-gilman¹⁹ J. Lien¹²² R. Lietava¹⁰¹ I. Likmeta¹¹⁷ B. Lim²⁵ S. H. Lim¹⁷
V. Lindenstruth³⁹ A. Lindner⁴⁶ C. Lippmann⁹⁸ D. H. Liu⁶ J. Liu¹²⁰ G. S. S. Liveraro¹¹² I. M. Lofnes²¹
C. Loizides⁸⁸ S. Lokos¹⁰⁸ J. Lömker⁶⁰ P. Loncar³⁴ X. Lopez¹²⁸ E. López Torres⁷ P. Lu^{98,121} F. V. Lugo⁶⁸
J. R. Luhder¹²⁷ M. Lunardon²⁸ G. Luparello⁵⁸ Y. G. Ma⁴⁰ M. Mager³³ A. Maire¹³⁰ E. M. Majerz²
M. V. Makariev³⁷ M. Malaev¹⁴² G. Malfattore²⁶ N. M. Malik⁹² Q. W. Malik²⁰ S. K. Malik⁹² L. Malinina^{143,a,f}
D. Mallick^{81,132} N. Mallick⁴⁹ G. Mandaglio^{31,54} S. K. Mandal⁸⁰ V. Manko¹⁴² F. Manso¹²⁸ V. Manzari⁵¹
Y. Mao⁶ R. W. Marcjan² G. V. Margagliotti²⁴ A. Margotti⁵² A. Marín⁹⁸ C. Markert¹⁰⁹ P. Martinengo³³
M. I. Martínez⁴⁵ G. Martínez García¹⁰⁴ M. P. P. Martins¹¹¹ S. Masciocchi⁹⁸ M. Masera²⁵ A. Masoni⁵³
L. Massacrier¹³² O. Massen⁶⁰ A. Mastroserio^{51,133} O. Matonoha⁷⁶ S. Mattiazzo²⁸ A. Matyja¹⁰⁸ C. Mayer¹⁰⁸
A. L. Mazuecos³³ F. Mazzaschi²⁵ M. Mazzilli³³ J. E. Mdhluhi¹²⁴ Y. Melikyan⁴⁴ A. Menchaca-Rocha⁶⁸
J. E. M. Mendez⁶⁶ E. Meninno¹⁰³ A. S. Menon¹¹⁷ M. Meres¹³ Y. Miake¹²⁶ L. Micheletti³³ D. L. Mihaylov⁹⁶
K. Mikhaylov^{142,143} D. Miśkowiec⁹⁸ A. Modak⁴ B. Mohanty⁸¹ M. Mohisin Khan^{16,g} M. A. Molander⁴⁴
S. Monira¹³⁷ C. Mordasini¹¹⁸ D. A. Moreira De Godoy¹²⁷ I. Morozov¹⁴² A. Morsch³³ T. Mrnjavac³³
V. Muccifora⁵⁰ S. Muhuri¹³⁶ J. D. Mulligan⁷⁵ A. Mulliri²³ M. G. Munhoz¹¹¹ R. H. Munzer⁶⁵
H. Murakami¹²⁵ S. Murray¹¹⁵ L. Musa³³ J. Musinsky⁶¹ J. W. Myrcha¹³⁷ B. Naik¹²⁴ A. I. Nambrath¹⁹
B. K. Nandi⁴⁸ R. Nania⁵² E. Nappi⁵¹ A. F. Nassirpour¹⁸ A. Nath⁹⁵ C. Natrass¹²³ M. N. Naydenov³⁷
A. Neagu²⁰ A. Negru¹¹⁴ E. Nekrasova¹⁴² L. Nellen⁶⁶ R. Nepeivoda⁷⁶ S. Nese²⁰ G. Neskovic³⁹ N. Nicassio⁵¹
B. S. Nielsen⁸⁴ E. G. Nielsen⁸⁴ S. Nikolaev¹⁴² S. Nikulin¹⁴² V. Nikulin¹⁴² F. Noferini⁵² S. Noh¹²
P. Nomokonov¹⁴³ J. Norman¹²⁰ N. Novitzky⁸⁸ P. Nowakowski¹³⁷ A. Nyanin¹⁴² J. Nystrand²¹ S. Oh¹⁸
A. Ohlson⁷⁶ V. A. Okorokov¹⁴² J. Oleniacz¹³⁷ A. Onnerstad¹¹⁸ C. Oppedisano⁵⁷ A. Ortiz Velasquez⁶⁶
J. Otwinowski¹⁰⁸ M. Oya⁹³ K. Oyama⁷⁷ Y. Pachmayer⁹⁵ S. Padhan⁴⁸ D. Pagano^{56,135} G. Paić⁶⁶
S. Paisano-Guzmán⁴⁵ A. Palasciano⁵¹ S. Panebianco¹³¹ H. Park¹²⁶ H. Park¹⁰⁵ J. Park⁵⁹ J. E. Parkkila³³
Y. Patley⁴⁸ B. Paul²³ H. Pei⁶ T. Peitzmann⁶⁰ X. Peng¹¹ M. Pennisi²⁵ S. Perciballi²⁵ D. Peresunko¹⁴²
G. M. Perez⁷ Y. Pestov¹⁴² V. Petrov¹⁴² M. Petrovici⁴⁶ R. P. Pezzi^{67,104} S. Piano⁵⁸ M. Pikna¹³ P. Pillot¹⁰⁴
O. Pinazza^{33,52} L. Pinsky¹¹⁷ C. Pinto⁹⁶ S. Pisano⁵⁰ M. Płoskoń⁷⁵ M. Planinic⁹⁰ F. Pliquett⁶⁵ M. G. Poghosyan⁸⁸
B. Polichtchouk¹⁴² S. Politano³⁰ N. Poljak⁹⁰ A. Pop⁴⁶ S. Porteboeuf-Houssais¹²⁸ V. Pozdniakov^{143,a}
I. Y. Pozos⁴⁵ K. K. Pradhan⁴⁹ S. K. Prasad⁴ S. Prasad⁴⁹ R. Preghenella⁵² F. Prino⁵⁷ C. A. Pruneau¹³⁸
I. Pshenichnov¹⁴² M. Puccio³³ S. Pucillo²⁵ Z. Pugelova¹⁰⁷ S. Qiu⁸⁵ L. Quaglia²⁵ S. Ragoni¹⁵ A. Rai¹³⁹
A. Rakotozafindrabe¹³¹ L. Ramello^{57,134} F. Rami¹³⁰ T. A. Rancien⁷⁴ M. Rasa²⁷ S. S. Räsänen⁴⁴ R. Rath⁵²
M. P. Rauch²¹ I. Ravasenga³³ K. F. Read^{88,123} C. Reckziegel¹¹³ A. R. Redelbach³⁹ K. Redlich^{80,h}
C. A. Reetz⁹⁸ H. D. Regules-Medel⁴⁵ A. Rehman²¹ F. Reidt³³ H. A. Reme-Ness³⁵ Z. Rescakova³⁸ K. Reygers⁹⁵
A. Riabov¹⁴² V. Riabov¹⁴² R. Ricci²⁹ M. Richter²⁰ A. A. Riedel⁹⁶ W. Riegler³³ A. G. Riffero²⁵
C. Ristea⁶⁴ M. V. Rodríguez³³ M. Rodríguez Cahuantzi⁴⁵ S. A. Rodríguez Ramírez⁴⁵ K. Røed²⁰
R. Rogalev¹⁴² E. Rogochaya¹⁴³ T. S. Rogoschinski⁶⁵ D. Rohr³³ D. Röhrich²¹ P. F. Rojas⁴⁵ S. Rojas Torres³⁶
P. S. Rokita¹³⁷ G. Romanenko²⁶ F. Ronchetti⁵⁰ A. Rosano^{31,54} E. D. Rosas⁶⁶ K. Roslon¹³⁷ A. Rossi⁵⁵
A. Roy⁴⁹ S. Roy⁴⁸ N. Rubini²⁶ D. Ruggiano¹³⁷ R. Rui²⁴ P. G. Russek² R. Russo⁸⁵ A. Rustamov⁸²
E. Ryabinkin¹⁴² Y. Ryabov¹⁴² A. Rybicki¹⁰⁸ H. Rytkonen¹¹⁸ J. Ryu¹⁷ W. Rzesza¹³⁷ O. A. M. Saarimaki⁴⁴
S. Sadhu³² S. Sadovsky¹⁴² J. Saetre²¹ K. Šafařík³⁶ P. Saha⁴² S. K. Saha⁴ S. Saha⁸¹ B. Sahoo⁴⁸ B. Sahoo⁴⁹
R. Sahoo⁴⁹ S. Sahoo⁶² D. Sahu⁴⁹ P. K. Sahu⁶² J. Saini¹³⁶ K. Sajdakova³⁸ S. Sakai¹²⁶ M. P. Salvan⁹⁸
S. Sambyal⁹² D. Samitz¹⁰³ I. Sanna^{33,96} T. B. Saramela¹¹¹ P. Sarma⁴² V. Sarritzu²³ V. M. Sarti⁹⁶
M. H. P. Sas³³ S. Sawan⁸¹ E. Scapparone⁵² J. Schambach⁸⁸ H. S. Scheid⁶⁵ C. Schiaua⁴⁶ R. Schicker⁹⁵
F. Schlepper⁹⁵ A. Schmah⁹⁸ C. Schmidt⁹⁸ H. R. Schmidt⁹⁴ M. O. Schmidt³³ M. Schmidt⁹⁴ N. V. Schmidt⁸⁸
A. R. Schmier¹²³ R. Schotter¹³⁰ A. Schröter³⁹ J. Schukraft³³ K. Schweda⁹⁸ G. Scioli²⁶ E. Scomparin⁵⁷
J. E. Seger¹⁵ Y. Sekiguchi¹²⁵ D. Sekihata¹²⁵ M. Selina⁸⁵ I. Selyuzhenkov⁹⁸ S. Senyukov¹³⁰ J. J. Seo⁹⁵
D. Serebryakov¹⁴² L. Serkin⁶⁶ L. Šerkšnytė⁹⁶ A. Sevcenco⁶⁴ T. J. Shaba⁶⁹ A. Shabetai¹⁰⁴ R. Shahoyan³³
A. Shangaraev¹⁴² B. Sharma⁹² D. Sharma⁴⁸ H. Sharma⁵⁵ M. Sharma⁹² S. Sharma⁷⁷ S. Sharma⁹²
U. Sharma⁹² A. Shatat¹³² O. Sheibani¹¹⁷ K. Shigaki⁹³ M. Shimomura⁷⁸ J. Shin¹² S. Shirinkin¹⁴² Q. Shou⁴⁰

Y. Sibiriak¹⁴², S. Siddhanta⁵³, T. Siemiarczuk⁸⁰, T. F. Silva¹¹¹, D. Silvermyr⁷⁶, T. Simantathammakul,¹⁰⁶
 R. Simeonov³⁷, B. Singh⁹², B. Singh,⁹⁶ K. Singh⁴⁹, R. Singh⁸¹, R. Singh⁹², R. Singh⁴⁹, S. Singh¹⁶,
 V. K. Singh¹³⁶, V. Singhal¹³⁶, T. Sinha¹⁰⁰, B. Sitar¹³, M. Sitta^{57,134}, T. B. Skaali,²⁰ G. Skorodumovs⁹⁵,
 M. Slupecki⁴⁴, N. Smirnov¹³⁹, R. J. M. Snellings⁶⁰, E. H. Solheim²⁰, J. Song¹⁷, C. Sonnabend^{33,98},
 J. M. Sonneveld⁸⁵, F. Soramel²⁸, A. B. Soto-hernandez⁸⁹, R. Spijkers⁸⁵, I. Sputowska¹⁰⁸, J. Staa⁷⁶, J. Stachel⁹⁵,
 I. Stan⁶⁴, P. J. Steffanic¹²³, S. F. Stiefelmaier⁹⁵, D. Stocco¹⁰⁴, I. Storehaug²⁰, P. Stratmann¹²⁷, S. Strazzi²⁶,
 A. Sturniolo^{31,54}, C. P. Stylianidis,⁸⁵ A. A. P. Suaide¹¹¹, C. Suire¹³², M. Sukhanov¹⁴², M. Suljic³³, R. Sultanov¹⁴²,
 V. Sumberia⁹², S. Sumowidagdo⁸³, S. Swain,⁶² I. Szarka¹³, M. Szymkowski¹³⁷, S. F. Taghavi⁹⁶, G. Taillepied⁹⁸,
 J. Takahashi¹¹², G. J. Tambave⁸¹, S. Tang⁶, Z. Tang¹²¹, J. D. Tapia Takaki¹¹⁹, N. Tapus,¹¹⁴ L. A. Tarasovicova¹²⁷,
 M. G. Tazila⁴⁶, G. F. Tassielli³², A. Tauro³³, A. Tavira García,¹³² G. Tejada Muñoz⁴⁵, A. Telesca³³, L. Terlizzi²⁵,
 C. Terrevoli¹¹⁷, S. Thakur⁴, D. Thomas¹⁰⁹, A. Tikhonov¹⁴², N. Tiltmann¹²⁷, A. R. Timmins¹¹⁷, M. Tkacik,¹⁰⁷
 T. Tkacik¹⁰⁷, A. Toia⁶⁵, R. Tokumoto,⁹³ K. Tomohiro,⁹³ N. Topilskaya¹⁴², M. Toppi⁵⁰, T. Tork¹³², V. V. Torres¹⁰⁴,
 A. G. Torres Ramos³², A. Trifiró^{31,54}, A. S. Triolo^{31,33,54}, S. Tripathy⁵², T. Tripathy⁴⁸, S. Trogolo³³,
 V. Trubnikov³, W. H. Trzaska¹¹⁸, T. P. Trzcinski¹³⁷, A. Tumkin¹⁴², R. Turrisi⁵⁵, T. S. Tveter²⁰, K. Ullaland²¹,
 B. Ulukutlu⁹⁶, A. Uras¹²⁹, M. Urioni¹³⁵, G. L. Usai²³, M. Vala,³⁸ N. Valle²², L. V. R. van Doremalen,⁶⁰
 M. van Leeuwen⁸⁵, C. A. van Veen⁹⁵, R. J. G. van Weelden⁸⁵, P. Vande Vyvre³³, D. Varga⁴⁷, Z. Varga⁴⁷,
 P. Vargas Torres,⁶⁶ M. Vasileiou⁷⁹, A. Vasiliev¹⁴², O. Vázquez Doce⁵⁰, O. Vazquez Rueda¹¹⁷, V. Vechernin¹⁴²,
 E. Vercellin²⁵, S. Vergara Limón,⁴⁵ R. Verma,⁴⁸ L. Vermunt⁹⁸, R. Vértesi⁴⁷, M. Verweij⁶⁰, L. Vickovic,³⁴
 Z. Vilakazi,¹²⁴ O. Villalobos Baillie¹⁰¹, A. Villani²⁴, A. Vinogradov¹⁴², T. Virgili²⁹, M. M. O. Virta¹¹⁸,
 V. Vislavicius,⁷⁶ A. Vodopyanov¹⁴³, B. Volkel³³, M. A. Völkl⁹⁵, S. A. Voloshin¹³⁸, G. Volpe³², B. von Haller³³,
 I. Vorobyev³³, N. Vozniuk¹⁴², J. Vrláková³⁸, J. Wan,⁴⁰ C. Wang⁴⁰, D. Wang,⁴⁰ Y. Wang⁴⁰, Y. Wang⁶,
 A. Wegrzynek³³, F. T. Weiglhofer,³⁹ S. C. Wenzel³³, J. P. Wessels¹²⁷, J. Wiechula⁶⁵, J. Wikne²⁰, G. Wilk⁸⁰,
 J. Wilkinson⁹⁸, G. A. Willems¹²⁷, B. Windelband⁹⁵, M. Winn¹³¹, J. R. Wright¹⁰⁹, W. Wu,⁴⁰ Y. Wu¹²¹, Z. Xiong,¹²¹
 R. Xu⁶, A. Yadav⁴³, A. K. Yadav¹³⁶, S. Yalcin⁷³, Y. Yamaguchi⁹³, S. Yang,²¹ S. Yano⁹³, E. R. Yeats,¹⁹ Z. Yin⁶,
 I.-K. Yoo¹⁷, J. H. Yoon⁵⁹, H. Yu,¹² S. Yuan,²¹ A. Yuncu⁹⁵, V. Zaccolo²⁴, C. Zampolli³³, F. Zanone⁹⁵,
 N. Zardoshti³³, A. Zarochentsev¹⁴², P. Závada⁶³, N. Zaviyalov,¹⁴² M. Zhalov¹⁴², B. Zhang⁶, C. Zhang¹³¹,
 L. Zhang⁴⁰, M. Zhang,⁶ S. Zhang⁴⁰, X. Zhang⁶, Y. Zhang,¹²¹ Z. Zhang⁶, M. Zhao¹⁰, V. Zhrebchevskii¹⁴²,
 Y. Zhi,¹⁰ C. Zhong,⁴⁰ D. Zhou⁶, Y. Zhou⁸⁴, J. Zhu^{6,55}, Y. Zhu,⁶ S. C. Zugravel⁵⁷ and N. Zurlo^{56,135}

(ALICE Collaboration)

¹A.I. Alikhanyan National Science Laboratory (Yerevan Physics Institute) Foundation, Yerevan, Armenia

²AGH University of Krakow, Cracow, Poland

³Bogolyubov Institute for Theoretical Physics, National Academy of Sciences of Ukraine, Kiev, Ukraine

⁴Bose Institute, Department of Physics and Centre for Astroparticle Physics and Space Science (CAPSS), Kolkata, India

⁵California Polytechnic State University, San Luis Obispo, California, USA

⁶Central China Normal University, Wuhan, China

⁷Centro de Aplicaciones Tecnológicas y Desarrollo Nuclear (CEADEN), Havana, Cuba

⁸Centro de Investigación y de Estudios Avanzados (CINVESTAV), Mexico City and Mérida, Mexico

⁹Chicago State University, Chicago, Illinois, USA

¹⁰China Institute of Atomic Energy, Beijing, China

¹¹China University of Geosciences, Wuhan, China

¹²Chungbuk National University, Cheongju, Republic of Korea

¹³Comenius University Bratislava, Faculty of Mathematics, Physics and Informatics, Bratislava, Slovak Republic

¹⁴COMSATS University Islamabad, Islamabad, Pakistan

¹⁵Creighton University, Omaha, Nebraska, USA

¹⁶Department of Physics, Aligarh Muslim University, Aligarh, India

¹⁷Department of Physics, Pusan National University, Pusan, Republic of Korea

¹⁸Department of Physics, Sejong University, Seoul, Republic of Korea

¹⁹Department of Physics, University of California, Berkeley, California, USA

²⁰Department of Physics, University of Oslo, Oslo, Norway

²¹Department of Physics and Technology, University of Bergen, Bergen, Norway

- ²²*Dipartimento di Fisica, Università di Pavia, Pavia, Italy*
- ²³*Dipartimento di Fisica dell'Università and Sezione INFN, Cagliari, Italy*
- ²⁴*Dipartimento di Fisica dell'Università and Sezione INFN, Trieste, Italy*
- ²⁵*Dipartimento di Fisica dell'Università and Sezione INFN, Turin, Italy*
- ²⁶*Dipartimento di Fisica e Astronomia dell'Università and Sezione INFN, Bologna, Italy*
- ²⁷*Dipartimento di Fisica e Astronomia dell'Università and Sezione INFN, Catania, Italy*
- ²⁸*Dipartimento di Fisica e Astronomia dell'Università and Sezione INFN, Padova, Italy*
- ²⁹*Dipartimento di Fisica 'E.R. Caianiello' dell'Università and Gruppo Collegato INFN, Salerno, Italy*
- ³⁰*Dipartimento DISAT del Politecnico and Sezione INFN, Turin, Italy*
- ³¹*Dipartimento di Scienze MIFT, Università di Messina, Messina, Italy*
- ³²*Dipartimento Interateneo di Fisica 'M. Merlin' and Sezione INFN, Bari, Italy*
- ³³*European Organization for Nuclear Research (CERN), Geneva, Switzerland*
- ³⁴*Faculty of Electrical Engineering, Mechanical Engineering and Naval Architecture, University of Split, Split, Croatia*
- ³⁵*Faculty of Engineering and Science, Western Norway University of Applied Sciences, Bergen, Norway*
- ³⁶*Faculty of Nuclear Sciences and Physical Engineering, Czech Technical University in Prague, Prague, Czech Prague, Czech*
- ³⁷*Faculty of Physics, Sofia University, Sofia, Bulgaria*
- ³⁸*Faculty of Science, P.J. Šafárik University, Košice, Slovak Republic*
- ³⁹*Frankfurt Institute for Advanced Studies, Johann Wolfgang Goethe-Universität Frankfurt, Frankfurt, Germany*
- ⁴⁰*Fudan University, Shanghai, China*
- ⁴¹*Gangneung-Wonju National University, Gangneung, Republic of Korea*
- ⁴²*Gauhati University, Department of Physics, Guwahati, India*
- ⁴³*Helmholtz-Institut für Strahlen- und Kernphysik, Rheinische Friedrich-Wilhelms-Universität Bonn, Bonn, Germany*
- ⁴⁴*Helsinki Institute of Physics (HIP), Helsinki, Finland*
- ⁴⁵*High Energy Physics Group, Universidad Autónoma de Puebla, Puebla, Mexico*
- ⁴⁶*Horia Hulubei National Institute of Physics and Nuclear Engineering, Bucharest, Romania*
- ⁴⁷*HUN-REN Wigner Research Centre for Physics, Budapest, Hungary*
- ⁴⁸*Indian Institute of Technology Bombay (IIT), Mumbai, India*
- ⁴⁹*Indian Institute of Technology Indore, Indore, India*
- ⁵⁰*INFN, Laboratori Nazionali di Frascati, Frascati, Italy*
- ⁵¹*INFN, Sezione di Bari, Bari, Italy*
- ⁵²*INFN, Sezione di Bologna, Bologna, Italy*
- ⁵³*INFN, Sezione di Cagliari, Cagliari, Italy*
- ⁵⁴*INFN, Sezione di Catania, Catania, Italy*
- ⁵⁵*INFN, Sezione di Padova, Padova, Italy*
- ⁵⁶*INFN, Sezione di Pavia, Pavia, Italy*
- ⁵⁷*INFN, Sezione di Torino, Turin, Italy*
- ⁵⁸*INFN, Sezione di Trieste, Trieste, Italy*
- ⁵⁹*Inha University, Incheon, Republic of Korea*
- ⁶⁰*Institute for Gravitational and Subatomic Physics (GRASP), Utrecht University/Nikhef, Utrecht, Netherlands*
- ⁶¹*Institute of Experimental Physics, Slovak Academy of Sciences, Košice, Slovak Republic*
- ⁶²*Institute of Physics, Homi Bhabha National Institute, Bhubaneswar, India*
- ⁶³*Institute of Physics of the Czech Academy of Sciences, Prague, Czech Republic*
- ⁶⁴*Institute of Space Science (ISS), Bucharest, Romania*
- ⁶⁵*Institut für Kernphysik, Johann Wolfgang Goethe-Universität Frankfurt, Frankfurt, Germany*
- ⁶⁶*Instituto de Ciencias Nucleares, Universidad Nacional Autónoma de México, Mexico City, Mexico*
- ⁶⁷*Instituto de Física, Universidade Federal do Rio Grande do Sul (UFRGS), Porto Alegre, Brazil*
- ⁶⁸*Instituto de Física, Universidad Nacional Autónoma de México, Mexico City, Mexico*
- ⁶⁹*iThemba LABS, National Research Foundation, Somerset West, South Africa*
- ⁷⁰*Jeonbuk National University, Jeonju, Republic of Korea*
- ⁷¹*Johann-Wolfgang-Goethe Universität Frankfurt Institut für Informatik, Fachbereich Informatik und Mathematik, Frankfurt, Germany*
- ⁷²*Korea Institute of Science and Technology Information, Daejeon, Republic of Korea*
- ⁷³*KTO Karatay University, Konya, Turkey*
- ⁷⁴*Laboratoire de Physique Subatomique et de Cosmologie, Université Grenoble-Alpes, CNRS-IN2P3, Grenoble, France*
- ⁷⁵*Lawrence Berkeley National Laboratory, Berkeley, California, USA*
- ⁷⁶*Lund University Department of Physics, Division of Particle Physics, Lund, Sweden*
- ⁷⁷*Nagasaki Institute of Applied Science, Nagasaki, Japan*
- ⁷⁸*Nara Women's University (NWU), Nara, Japan*
- ⁷⁹*National and Kapodistrian University of Athens, School of Science, Department of Physics, Athens, Greece*
- ⁸⁰*National Centre for Nuclear Research, Warsaw, Poland*
- ⁸¹*National Institute of Science Education and Research, Homi Bhabha National Institute, Jatni, India*

- ⁸²National Nuclear Research Center, Baku, Azerbaijan
- ⁸³National Research and Innovation Agency - BRIN, Jakarta, Indonesia
- ⁸⁴Niels Bohr Institute, University of Copenhagen, Copenhagen, Denmark
- ⁸⁵Nikhef, National institute for subatomic physics, Amsterdam, Netherlands
- ⁸⁶Nuclear Physics Group, STFC Daresbury Laboratory, Daresbury, United Kingdom
- ⁸⁷Nuclear Physics Institute of the Czech Academy of Sciences, Husinec-Řež, Czech Republic
- ⁸⁸Oak Ridge National Laboratory, Oak Ridge, Tennessee, USA
- ⁸⁹Ohio State University, Columbus, Ohio, USA
- ⁹⁰Physics department, Faculty of science, University of Zagreb, Zagreb, Croatia
- ⁹¹Physics Department, Panjab University, Chandigarh, India
- ⁹²Physics Department, University of Jammu, Jammu, India
- ⁹³Physics Program and International Institute for Sustainability with Knotted Chiral Meta Matter (SKCM2), Hiroshima University, Hiroshima, Japan
- ⁹⁴Physikalisches Institut, Eberhard-Karls-Universität Tübingen, Tübingen, Germany
- ⁹⁵Physikalisches Institut, Ruprecht-Karls-Universität Heidelberg, Heidelberg, Germany
- ⁹⁶Physik Department, Technische Universität München, Munich, Germany
- ⁹⁷Politecnico di Bari and Sezione INFN, Bari, Italy
- ⁹⁸Research Division and ExtreMe Matter Institute EMMI, GSI Helmholtzzentrum für Schwerionenforschung GmbH, Darmstadt, Germany
- ⁹⁹Saga University, Saga, Japan
- ¹⁰⁰Saha Institute of Nuclear Physics, Homi Bhabha National Institute, Kolkata, India
- ¹⁰¹School of Physics and Astronomy, University of Birmingham, Birmingham, United Kingdom
- ¹⁰²Sección Física, Departamento de Ciencias, Pontificia Universidad Católica del Perú, Lima, Peru
- ¹⁰³Stefan Meyer Institut für Subatomare Physik (SMI), Vienna, Austria
- ¹⁰⁴SUBATECH, IMT Atlantique, Nantes Université, CNRS-IN2P3, Nantes, France
- ¹⁰⁵Sungkyunkwan University, Suwon City, Republic of Korea
- ¹⁰⁶Suranaree University of Technology, Nakhon Ratchasima, Thailand
- ¹⁰⁷Technical University of Košice, Košice, Slovak Republic
- ¹⁰⁸The Henryk Niewodniczanski Institute of Nuclear Physics, Polish Academy of Sciences, Cracow, Poland
- ¹⁰⁹The University of Texas at Austin, Austin, Texas, USA
- ¹¹⁰Universidad Autónoma de Sinaloa, Culiacán, Mexico
- ¹¹¹Universidade de São Paulo (USP), São Paulo, Brazil
- ¹¹²Universidade Estadual de Campinas (UNICAMP), Campinas, Brazil
- ¹¹³Universidade Federal do ABC, Santo Andre, Brazil
- ¹¹⁴Universitatea Nationala de Stiinta si Tehnologie Politehnica Bucuresti, Bucharest, Romania
- ¹¹⁵University of Cape Town, Cape Town, South Africa
- ¹¹⁶University of Derby, Derby, United Kingdom
- ¹¹⁷University of Houston, Houston, Texas, USA
- ¹¹⁸University of Jyväskylä, Jyväskylä, Finland
- ¹¹⁹University of Kansas, Lawrence, Kansas, USA
- ¹²⁰University of Liverpool, Liverpool, United Kingdom
- ¹²¹University of Science and Technology of China, Hefei, China
- ¹²²University of South-Eastern Norway, Kongsberg, Norway
- ¹²³University of Tennessee, Knoxville, Tennessee, USA
- ¹²⁴University of the Witwatersrand, Johannesburg, South Africa
- ¹²⁵University of Tokyo, Tokyo, Japan
- ¹²⁶University of Tsukuba, Tsukuba, Japan
- ¹²⁷Universität Münster, Institut für Kernphysik, Münster, Germany
- ¹²⁸Université Clermont Auvergne, CNRS/IN2P3, LPC, Clermont-Ferrand, France
- ¹²⁹Université de Lyon, CNRS/IN2P3, Institut de Physique des 2 Infinis de Lyon, Lyon, France
- ¹³⁰Université de Strasbourg, CNRS, IPHC UMR 7178, F-67000 Strasbourg, France, Strasbourg, France
- ¹³¹Université Paris-Saclay, Centre d'Etudes de Saclay (CEA), IRFU, Département de Physique Nucléaire (DPHN), Saclay, France
- ¹³²Université Paris-Saclay, CNRS/IN2P3, IJCLab, Orsay, France
- ¹³³Università degli Studi di Foggia, Foggia, Italy
- ¹³⁴Università del Piemonte Orientale, Vercelli, Italy
- ¹³⁵Università di Brescia, Brescia, Italy
- ¹³⁶Variable Energy Cyclotron Centre, Homi Bhabha National Institute, Kolkata, India
- ¹³⁷Warsaw University of Technology, Warsaw, Poland
- ¹³⁸Wayne State University, Detroit, Michigan, USA
- ¹³⁹Yale University, New Haven, Connecticut, USA

¹⁴⁰*Yonsei University, Seoul, Republic of Korea*

¹⁴¹*Zentrum für Technologie und Transfer (ZTT), Worms, Germany*

¹⁴²*Affiliated with an institute covered by a cooperation agreement with CERN*

¹⁴³*Affiliated with an international laboratory covered by a cooperation agreement with CERN*

^aDeceased.

^bAlso at Max-Planck-Institut für Physik, Munich, Germany.

^cAlso at Italian National Agency for New Technologies, Energy and Sustainable Economic Development (ENEA), Bologna, Italy.

^dAlso at Dipartimento DET del Politecnico di Torino, Turin, Italy.

^eAlso at Yildiz Technical University, Istanbul, Türkiye.

^fAlso at An institution covered by a cooperation agreement with CERN.

^gAlso at Department of Applied Physics, Aligarh Muslim University, Aligarh, India.

^hAlso at Institute of Theoretical Physics, University of Wrocław, Poland.